Literature review of numerical simulation and optimisation of the shot peening process

Jun S Chen[1] (iD), Dawood A Desai[1], Stephan P Heyns[2] and Francesco Pietra[3]

Abstract

This work provides a comprehensive review of numerical simulation and optimisation of the shot peening found in the existing literature over the past 10 years. The review found that the developed numerical models coupling finite elements with discrete elements became increasingly mature and showed their advantages in incorporating flow behaviour and randomness of shots. High emphasis must be placed on the constitutive equations of target material where its strain-rate sensitivity, cyclic behaviour and Bauschinger effects are recommended to be incorporated in the numerical material model simultaneously since considering one of them in isolation may lead to unreliable distribution of residual stresses. Furthermore, material hardening is a critical benefit of shot peening; however, it has not received its deserved attention from the existing investigations, neither in simulation nor in optimisation. The study found that intensity and coverage are two critical control parameters recommended to be constraints for optimisation of shot peening. Finally, this work also found that developed heuristic algorithms, such as genetic algorithms have recently showed their advantages for searching optimal combinations of peening parameters. It is plausible that in the near future, the synergy of combining these algorithms with approximation models can be expected to gain more attention by researchers.

Keywords

Literature review, shot peening, numerical simulation, optimisation, algorithm

Introduction

Shot peening (SP), as a surface treatment process, is frequently used to enhance the fatigue life of metallic components[1,2] in the manufacturing industry, since it produces compressive residual stresses (CRSs) on the peened surface to delay initiation of fatigue failure and retard its propagation.[3] On the contrary, this surface treatment also induces surface roughness and causes cold working of the peened component.[3] These two effects are detrimental to the fatigue life of the component. Furthermore, the SP process is influenced by several continuous and discrete parameters[4] which have deterministic influences on its effectiveness.[5] Among some of these parameters, interactions exist between each other.[6] Most importantly, its potential to enhance fatigue life of components depends on the reasonable

[1]Faculty of Engineering and the Built Environment, Tshwane University of Technology, Pretoria, South Africa
[2]Faculty of Engineering and the Built Environment, University of Pretoria, Pretoria, South Africa
[3]School of Mechanical, Industrial and Aeronautical Engineering, University of the Witwatersrand, Johannesburg, South Africa

Corresponding author:
Jun S Chen, Faculty of Engineering and the Built Environment, Tshwane University of Technology, Pretoria 0001, Gauteng, South Africa.
Email: newbonchen@hotmail.com

application of these influential parameters.[1,7] In other words, inappropriately specifying these influential parameters could reduce the benefits of CRS induced by SP. Since SP has many influential parameters, and produces both detrimental and beneficial effects, many investigations have been conducted to study this surface treatment process. These investigations include examining the material behaviour of its target components,[8] adjusting its influential parameters,[9,10] controlling its detrimental effects[11,12] and simultaneously enhancing the beneficial effects arising from the induced CRS. In addition, compared to physical experimentation, numerical methods were increasingly used since it is time-saving and economical. As research into SP attracts increasing attention, it is crucial to provide a global insight into this field by reviewing the relevant literature. Hence, this article provides an extensive and critical review of the available literature on both numerical simulation and optimisation of SP in the past 10 years or so.

SP and its influential parameters

SP

SP is a cold working process and a surface finish treatment often applied to improving the fatigue life of metallic components[13] in the aero,[14] power generation, automotive and biomedical industries.[3] It is essentially a process where one solid sphere impacts another solid surface,[15] as shown in Figure 1. During this process, the target deforms leading to compression in its surface layer. The process of the deformation and the compression of the target material are illustrated as follows.

During the SP process, the shot strikes the target (plate surface) acting as a tiny peening hammer, which forces the material of the plate at the impact centre to flow away. Some flow patterns create space for the newly formed indentation, while the other flow patterns form a ridge around the indentation. The indentation and the surrounding ridge are the two components of an impact.[16] Simultaneously, as the material flows away, the surface layer yields in tension due to the creation of the indentations, while the material below the surface layer tries to restore its original shape. Subsequently, a layer highly stressed in compression is produced[16] exhibiting CRS.

Influential parameters and responses to SP

SP is determined by many influential parameters which can be classified into three groups, namely, peening medium, peening device and workpiece.[17,18] Figure 2 depicts these three groups and the corresponding SP products, namely, residual stress, surface roughness and material hardening. In line with the significance of their influences, only the main parameters, such as
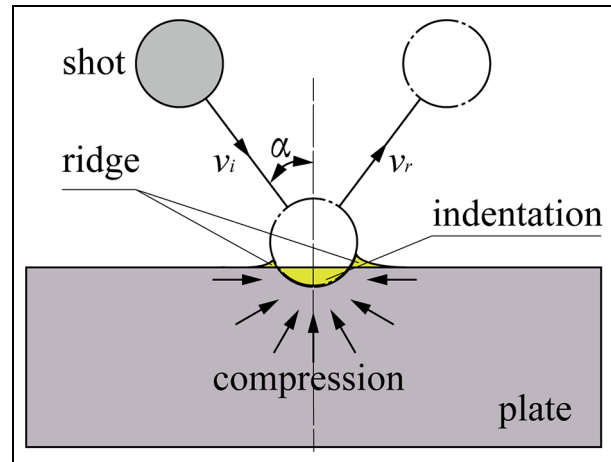

Figure 1. Schematic diagram of formation of CRS. The shot moves at a constant velocity, v_i, to the plate with a certain incidence angle, α. After its impingement on the target surface, it re-bounces at a smaller velocity, v_r.

radius of the shot, initial velocity of the shot, incidence angle, coverage (or exposure time), behaviour of the material of the shot and the workpiece, are considered for research purposes.[4,19] However, in industry, most of the parameters hereof are not controllable or hard to control directly. Hence, only two parameters, namely, Almen intensity and peening coverage, are used both to standardise and control SP by a measurement of Almen arc height[4] and to assure the repeatability of the process.[17]

Numerical simulation of SP

Numerical models

Numerical models are widely used to acquire further knowledge of SP and are applied as a substitute for physical models in optimisation runs due to their time-saving property which reduces economic cost.[20,21] Besides the summary of models cited in Zimmermann and Klemenz,[22] the developed numerical models with information about their materials and solvers are shown in Table 1 below.

Critical analysis of two-dimensional, three-dimensional and finite element–discrete element models

As depicted in Table 1, two-dimensional (2D) models account for a small percentage among the different types of available models due to their drawbacks.[22] The drawbacks are that residual stresses in 2D models are theoretically larger than those from their corresponding experiments, and that they are not capable of taking coverage into account. Only few investigators used
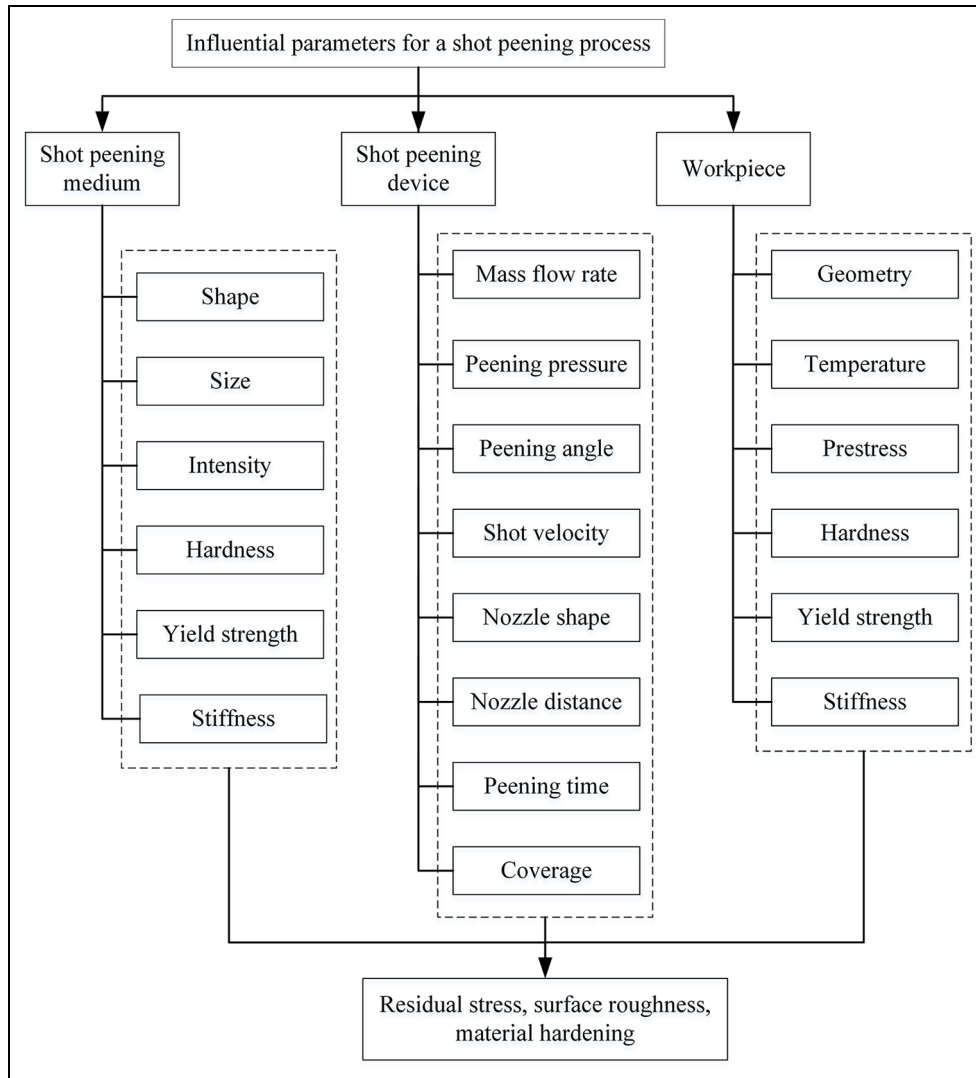
Figure 2. Influential parameters and products of SP.

them mainly as references to three-dimensional (3D) models.[23–25] For such applications, the 2D models are usually axisymmetric,[23,24] utilising single impact[23,24] and very fine meshes[23,24] with even fewer investigations[26,27] using them as counterparts to physical experiments. On the contrary, 3D models nowadays have become the standard for SP simulation due to their capability to overcome the drawbacks of 2D models mentioned above. However, 3D models are time-consuming[22] and have difficulties in simulating flow of large number of discrete shots impinging on a surface.[28] Interestingly, these shortfalls have led to the increasing application of a different type of model,[21,27,29] namely, a model coupling finite elements with discrete elements (FEM-DEM). One such model is implicated in the investigation by Jebahi et al.[21]

Furthermore, this type of model has become increasingly mature in terms of simulation of SP since 2010, especially from 2015 till now where discrete elements are employed in the generation of large number of shots[30,31] and the description of their flow behaviour.[30,31] These shots are assumed rigid and thus their substitution of finite element shots can definitely reduce computational cost under the same hardware conditions[19,29] which is extremely beneficial for optimisation of SP[28] where thousands of iterations are required with each iteration engaging the numerical model once. With this advantage at hand, it has now become possible for considering both shot–shot and shot–target interactions even if there are more than 4000 shots.[27] One interesting representative work considered the interaction between shots themselves, shot–target interaction and the usage of different shot sizes employing a large number of shots as shown in Figure 3.[27] However, a subsequent contrary investigation reported that the consideration of shot–shot interactions in a DEM model may still
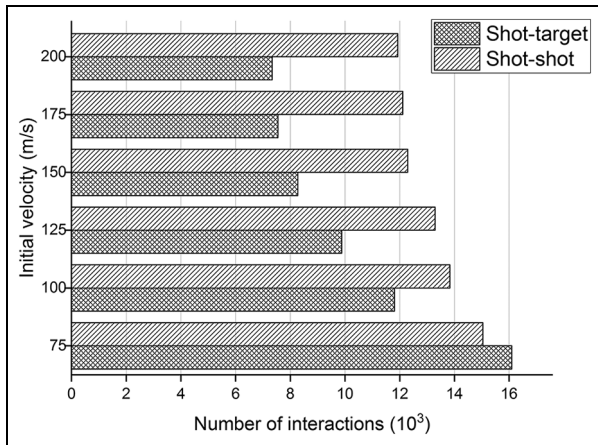
Figure 3. Number shot–shot and shot–target interaction for different shot diameters.
Adapted from Miao et al.[27]

result in unaffordable computational costs.[21] The reason cited were differences in the approach in creation of the discrete elements where Miao et al.[27] created the discrete element shots in EDEM code (a commercial software) and then conducted an analysis before combining the DEM with FEM, while generation of discrete element shots by Jebahi et al.[21] were to simulate flow without employing EDEM. Interestingly, the simulation results of the latter were validated experimentally showing an 8% discrepancy between the maximum residual stress values, while the distribution of the numerical residual stress and that of the experimental residual stresses were highly consistent with each other.

Apart from the advantages aforementioned, DEMs cannot consider the deformation of shots as the shots created by finite element method combined with discrete element method are rigid bodies,[27] so that its application would be appropriate under the assumption that rigid shots (shots are deformable in real SP) do not lead to unreliable residual stresses. Fortunately, this assumption is the general case in real SP.[32]

Dynamic explicit versus static implicit analysis

Both dynamic explicit and quasi-static implicit analyses were presented in the literature (as shown in Table 1) for different simulation purposes in line with their corresponding advantages. As for SP, a static analysis cannot specify the displacement of shots (projectiles) and the indentation of the shot into target material,[22] and neither can it independently consider the inherent dynamic features,[10,23] including initial velocity as boundary conditions (BCs),[22] inertia effects[30] and stress wave propagation.[33–38]

These limitations has led to the wide usage of the dynamic explicit procedure in simulation of SP. Table 1 shows that many investigations used the dynamic procedure or combined dynamic with static procedure to conduct their simulations, implying that the dynamic procedure was used to analyse the impact process (dynamic) of SP and sequentially employing the static procedure to analyse the reaction of the target material after impact (static).[23,29] The reason for this methodology could be that dynamic explicit procedures are better suitable for fast non-linear contact with higher efficiency and robustness because it adopts explicit time integration without either iterative calculations or the generation of tangent stiffness matrixes.[30,31] Note that the dynamic explicit procedure causes stress waves to propagate which usually lead to stress oscillation, although this problem could be well solved by many numerical methods. These methods include averaging the stress oscillation,[39] adopting damping techniques,[38] adding non-reflecting BCs as in LS-DYNA,[36] employing infinite elements in ABAQUS[40,41] software or using quasi-static analysis subsequent to the dynamic impact simulation.[22]

However, single impact simulations with dynamic models usually take much longer time than quasi-static models,[3] while this problem could be eradicated by the abovementioned method, that is, combining dynamic procedure with the static procedure. However, quasi-static analysis is simpler than a dynamic analysis in terms of information it is capable of producing. Therefore, it is appropriate to use quasi-static models as an aid or complementary procedure dealing with static aspects of SP only.[23,29] For example, investigations done by Kang et al.,[23] Sun and Zhang et al.,[36] Gariepy et al.[42] and Amarchinta et al.[43] used static analysis after a dynamic procedure to rapidly stabilise the model so as to avoid the long computation procedure for dynamic analysis to reach a steady state. Edward et al.[29] also used it in ANSYS software to save time as well and additionally to save hard disc space; and Frija et al.[15] used it in the simplification of SP simulation models.

Target material

Material modelling. Different material models are used for the elastoplastic target materials with different material-hardening behaviours, typically isotropic,[21,23,35,44] kinematic[45–47] and combined isotropic and kinematic hardening.[41,48,49] The isotropic model is employed for materials whose yield surface size changes uniformly in different directions so that the corresponding yield stresses change when plastic deformation occurs. It should be noted that isotropic models are generally appropriate where the

Table 1. Overview of numerical models for SP optimisation.

Author(s)	Solver	Method	Dim.	Target material modelling				Shot material modelling		Frc.	DEM
				Def.	Hdn.	$f(\dot{\varepsilon})$	$f(T)$	Def.	No.		
Klemenz et al.[48]	Abaqus, Fortran	Dynamic	3D	el. pl.	com.	Yes	Yes	Rigid	40	Yes	No
Miao et al.[44]	MATLAB, Ansys, LS-DYNA	Dynamic	3D	el. pl.	iso.	No	–	Rigid	6, 12, 24, 48, 96	Yes	No
Shivpuri et al.[35]	Abaqus	Dynamic	3D	el. pl.	iso.	Yes	Yes	Rigid	1, 2, 3, 4, 5, 6	Yes	No
Bagherifard et.al.[55]	Abaqus	Dynamic	3D	el. pl.	com.	Yes	No	el.	1, 134	Yes	No
Bhuvaraghan et al.[19]	DMEM, Abaqus	Dynamic	3D	el. pl.	–	Yes	–	Rigid	Multiple	No	Yes
Kang et al.[23]	Abaqus	Static, dynamic	2D, 3D	el. pl.	iso.	Yes	–	Rigid	1, multiple	No	–
Kim et al.[79]	Abaqus	Dynamic	3D	el. pl.	–	Yes	Yes	Rigid, el. pl.	1, 4, 16, 20	Yes	No
Gariepy et al.[42]	Abaqus	Dynamic	3D	el. pl.	com.	No	Yes	Rigid	1, 48	Yes	–
Kim et al.[24]	Abaqus	Dynamic	2D, 3D	el. pl.	–	Yes	Yes	Rigid, el. pl.	1, multiple	Yes	–
Miao et al.[27]	ANSYS, LS-DYNA	Dynamic	3D	el. pl.	iso.	No	–	Rigid	48	–	–
Mylonas and Labeas[45]	PAM Visual-Crash	Dynamic	3D	el. pl.	knm.	Yes	–	Rigid	7, 10, 30	–	No
Bagherifard et al.[46]	Abaqus	Dynamic	3D	el. pl.	knm.	No	–	el.	1, multiple	–	No
Bagherifard et al.[20]	Abaqus, Python	Dynamic	3D	el. pl.	knm.	No	–	el.	Multiple	–	No
Kim et al.[34]	Abaqus	Dynamic	3D	el. pl.	iso.	Yes	Yes	Rigid, el. pl.	1, 7n	Yes	No
Kim et al.[31]	Abaqus	Dynamic	3D	el. pl.	–	Yes	Yes	el. pl.	4, 8, 12, 16	Yes	No
Kim et al.[33]	Abaqus	Dynamic	3D	el. pl.	–	Yes	Yes	Rigid, el. pl.	1, multiple	Yes	No
Gangaraj et al.[78]	Abaqus	Dynamic	3D	el. pl.	iso.	Yes	No	el.	1, multiple	Yes	No
Mann et al.[49]	Abaqus	Dynamic	3D	el. pl.	com.	–	–	Rigid	1, multiple	–	No
Romero-Angeles et al.[26]	Ansys	Dynamic	2D	el. pl.	knm.	Yes	–	Rigid	7	–	No
Sun and Zhang[36]	Abaqus	Dynamic	2D, 3D	el. pl.	iso.	Yes	Yes	Rigid	9	–	No
Hassani-Gangaraj et al.[25]	Abaqus	Dynamic	2D, 3D	el. pl.	iso.	Yes	Yes	el. pl.	1, multiple	Yes	No
Ahmadi et al.[80]	Abaqus, EDEM	Dynamic	3D	el. pl.	knm., iso.	Yes	–	Rigid	1	Yes	No
Miao et al.[27]	EDEM, Abaqus	Dynamic	3D	el. pl.	–	–	–	Rigid	1, multiple	Yes	Yes
Edward et al.[29]	EDEM, Ansys	Static, dynamic	3D	el. pl.	iso.	Yes	–	Rigid	Multiple	–	Yes
Jebahi et al.[21]	Abaqus, Python	Dynamic	3D	el. pl.	iso.	Yes	Yes	Rigid	Multiple	Yes	Yes
Klemenz et al.[47]	Abaqus	Dynamic	3D	el. pl.	knm.	No	Yes	el.	1, 27	Yes	No
Xie et al.[90]	Ansys, LS-DYNA	Dynamic	3D	el. pl.	–	Yes	–	Rigid	1, 4	–	No

Dim. = dimension; – = unknown; Def. = deformable; Hdn = hardening; Frc. = friction; DEM = discrete element method; el. = elastic; pl. = plastic; iso. = isotropic; knm = kinematic; com. = combined isotropic and kinematic; multiple = when the number of shots is more than 1 while its concrete number remains known; $7n = 7 \times n$, where $n = 1, 2, 3, 4, 5, 6, 7$.
DEM in this table means using flowing particles for generation of shots/projectiles.

cyclic loads are monotonic and Bauschinger effects do not occur.[8] The kinematic material model is used for modelling the cyclic loading of a material with a constant hardening rate which does not consider strain-rate sensitivity (SRS), while the combination of these models are generally used for modelling both cyclic loading of a material and its non-linear isotropic–kinematic hardening[50] behaviour. In addition, the Johnson–Cook material model is widely applied for isotropic hardening[35] representation.

Besides general elasticity and plasticity of the material, SRS, cyclic behaviour and Bauschinger effects are three important factors influencing the distribution of residual stresses. However, some researchers do not consider SRS because the material used has low rate-dependant sensitivity[42] or the effects of sensitivity in their investigation is negligible.[47] Some data of the sensitivity–stress relation for mild steels was presented by Campbell and Ferguson.[51] However, it has been proven that SRS of the target materials has considerable influences on the distribution of residual stresses[41,52–56] since the target materials in SP generally undergo high strain rates. These influences were exhibited by many investigations[37,45,57] through comparisons of strain-rate-sensitive constitutive relationships. One interesting work conducted by Meguid et al.[32] demonstrated a typical curve of the change tendency of strain rate along with time during a SP process, as shown in Figure 4.

There are typically two popular formulae describing constitutive relations capable of incorporating the strain-rate implicitly. The first formula is the Cowper–Symonds power law proposed by Cowper and Symonds,[58] as described in equation (1). It must be noted that this equation is used to indirectly incorporate the strain rate rather than SRS. This power law was also used by many other investigations[33,37,45,59–61] to incorporate the effect of strain rate in SP simulations. The two constants, D and k, have different values, respectively, corresponding to different materials, for example, $D = 2 \times 10^4$ and $k = 3$ for a titanium alloy[59] while $D = 2.5 \times 10^6$ and $k = 6$ for AISI 4340[34,62]

$$\sigma_f = \sigma_0 \left(1 + \left(\frac{\dot{\varepsilon}}{D} \right)^{\frac{1}{k}} \right) \quad (1)$$

where σ_f is the stress, σ_0 is the yield stress for $\dot{\varepsilon} = 0$, $\dot{\varepsilon}$ is the strain rate, and D (with the unit s^{-1}) and k are the constants.

The second formula is the well-known Johnson–Cook function[63] described in equation (2). An investigation[64] shows that this equation is capable of predicting the stress–strain relationship well and is widely applied in SP for modelling the target material considering SRS. It is important to note that that these
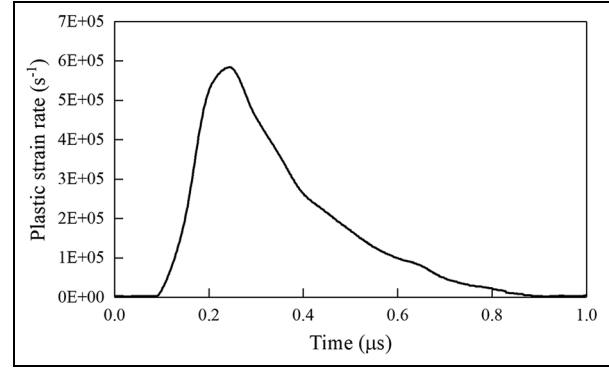

Figure 4. Equivalent plastic strain-rate time history during the initial stage of peening for a point 65 μm beneath the target surface on the centreline of the first shot.
Adapted from Meguid et al.[32]

two formulae are used to represent strain-rate implicitly rather than evaluate SRS.

$$\sigma_f = (A + B\varepsilon^n) \left(1 + C\ln\left(\frac{\dot{\varepsilon}}{\dot{\varepsilon}_0}\right) \right) \left[1 - \left(\frac{T - T_0}{T_m - T_0} \right)^m \right] \quad (2)$$

where ε and $\dot{\varepsilon}_0$ are the strain and a relevant constant with the value $1s^{-1}$, respectively; T, T_0 and T_m are, respectively, the temperature, the reference temperature, and the melting temperature; σ_f is the stress; and the others are material parameters.

The above two equations support the observations that stresses decrease with a reduction in strain rates. Through both experiment and simulation, Klemenz et al.[48] presented that, lower strain rates corresponded to lower flow stresses under the same temperature conditions. It was also reported that the magnitude of maximum residual stress beneath the impact centre in the target material was smaller than that of maximum residual stress produced without consideration of SRS.[53] Hence, it can be seen that SRS is material-specific and has significant influence on target materials which are strain-rate sensitive.

Cyclic behaviour of the target material also has influential effects on the distribution of the induced residual stresses.[8] Both Sanjurjo et al.[8] and Klemenz et al.[41] found that exclusion of cyclic behaviour to a material model resulted in overestimation of residual stresses. In support of this, another investigation showed that the surface regions of the target material experienced arbitrary cyclic loadings and these loadings must not be neglected[53] since they could cause relaxation to the residual stresses induced by previous impacts.[65,66] In multiple impact simulation, the target material encounters repeated impacts, hence cyclic loading occurs.[8] The mechanism to how cyclic behaviour affects the distribution of residual stresses is that the induced residual

stresses can be relaxed by subsequent cyclic loadings that the target material undergoes during SP. Some research also showed congruent results. For example, experimental work by Gariepy et al.[42] showed differences in results with the consideration of cyclic behaviour and that without it. In addition, most materials ignoring cyclic behaviour possess elastoplastic hardening, as shown in Table 1, while those considering it display visco-plastic hardness behaviour.[8,41,48,53,67]

As aforementioned, the target material undergoes cyclic loading conditions[53] caused by multiple impacts in SP.[8] This cyclic loading may precipitate Bauschinger effects which redistributes the residual stresses if prior loading exists.[26] It was found that results ignoring Bauschinger effects lead to an overestimation of residual stress[22] and this could be validated by the differences between residual stresses produced by isotropic material models (not allowing for Bauschinger effects) and kinematic models (allowing for Bauschinger effects).[68] One possible explanation is that the Bauschinger effect has the potential to cause stress relaxation.[69] In order to investigate this effect, one interesting study conducted by Urriolagoitia-Sosa et al.[70] experimentally induced Bauschinger effects and proposed a strain-gauge-based method capable of measuring the resulting residual stresses. Sanjurjo et al.[8] drew a conclusion from the investigation by Bannantine[71] that Bauschinger effects should be taken into account if the kinematic hardening material model should be employed. Hence, it can be concluded that Bauschinger effect has significant influence on the residual stresses induced by SP and must be considered.

In order to investigate the influences of the above factors, Klemenz et al.[53] compared the residual stresses obtained from their numerical models (one isotropic hardening and one combined isotropic and kinematic hardening) to physical experiments. The comparison showed that the results from the combined isotropic–kinematic material model were in good agreement with the experimental results. The relevant material model was later introduced in the investigation conducted by Klemenz et al.[48] in an expanded way. As the above discussion in this section shows, the residual stresses would be overestimated when only considering SRS; however, they would be underestimated when only considering the cyclic loading effects and Bauschinger effects.[8] In general, the target materials in SP are strain-rate sensitive in most cases and undergo cyclic loadings. Therefore, it is appropriate to employ an elastic–viscous–plastic combined hardening material model when taking all these factors into account.[48]

Thermal effects. Although SP is a cold work process, it still produces heat during impacts between the shots and the target material.[72] Harada and Mori[73] showed
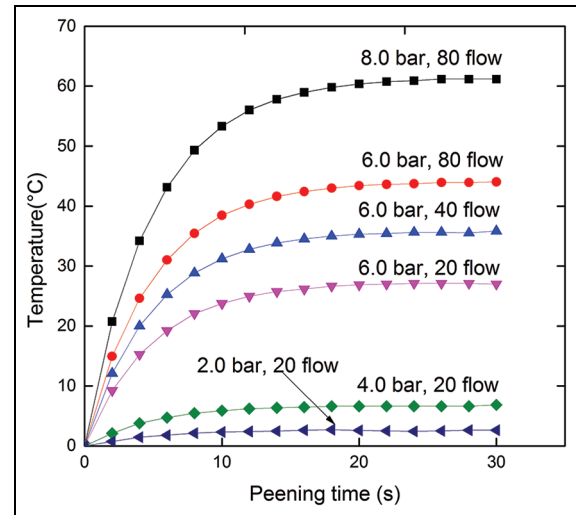

Figure 5. Heating curves for *N* strip during peening using S170 shot.
Adapted from Kirk.[74]

that the temperature alterations could affect the profile of residual stresses. Furthermore, the temperature increase could amount to 63°C when the cast steel shots reached the velocity of 50 m/s with a shot diameter of 2 mm under a so-called 'adiabatic' assumption. This observation was reported by Kirk[74] who conducted a series of tests with different air pressures ranging from 2 to 8 bar with three different flow rates of 20 flow (0.49 kg/min), 40 flow (0.88 kg/min) and 80 flow (1.58 kg/min) in the same investigation, as shown in Figure 5. Rouquette et al.[75] found that surface residual stress could have a maximum of 150 MPa discrepancy between models with and without consideration of thermal effects, while thermal properties just affected the magnitude of residual stress but not the distribution trend along the depth at impact centre of the target material. Apart from finding discrepancies of maximum 319 MPa of surface residual stresses, Hu et al.[76] further found that there were differences (maximum 1.66 mm) for arc height of Almen strips between models with and without consideration of thermal effects.

It can be seen that the residual stress decreases when considering thermal effects of the target material when employing either the Johnson–Cook model (see equation (2)) or the model proposed by Kocks et al.[77] During each impact, a fraction of the kinetic energy of shot is transformed into heat energy which causes surface temperature rises.[74] This increase would definitely lead to a decrease in the corresponding flow stress σ_f according to the two just-mentioned equations. In order to see an obvious temperature rise, Kirk[74] departed from conventional SP to deliberately increase the surface temperature with severe impacts at very high velocity of 200 m/s with a very small shot diameter of

50 μm. Hence, it was ascertained that the induced residual stresses undergo a kind of stress relaxation caused by thermal loadings generated during impacts.

Contrary to these researchers[73,75,76] who concluded that thermal effects should be considered, many others insisted on not considering thermal effects. Kirk[74] reported that the increase in temperature was only a few degrees; and again ElTobgy et al.[38] concluded that the temperature rise was small in their model and that the corresponding thermal effects were not necessary by a comparison between results obtained from a model with and without consideration of thermal effects. Some other researchers such as Bagherifard et al.[55] and Gangaraj et al.[78] just neglected thermal effects in their investigations while they still obtained simulation results consistent with those from experiments. These contrary observations might arise based on the different parameters applied in the models. However, as discussed above, the temperature rise is affected by shot velocity, shot diameter, exposure time and so on.[74] Thus, whether to consider thermal effects in a model depends on whether the applied parameters are severe enough to cause thermal relaxation.

Friction. Many investigations have been carried out using Coulomb's friction models and modified versions of them without any consistent conclusions on the influence of friction on the induced residual stresses being reached. Some researchers argued that friction had significant influence on the induced residual stresses,[21,24,34,41,42,48,62,79,80] therefore most investigations took friction into account through application of friction models among which Coulomb's friction model was widely applied.[25,44,47,55,78] In these studies, some researcher hypothesised that there would be a threshold above which friction coefficient had no effects on residual stresses while under, it had significant effects. Taking the investigation by Kim et al.[33] as an example, effects of friction on residual stresses on the surface and beneath were observed and a threshold was assumed, as shown in Figure 6. The maximum residual stresses with respect to different shots, that is, rigid shot, plastic shot and elastic shot, increase with the increase in friction coefficient from 0 to 0.3, while no further changes occur when the friction coefficient ranges from 0.3 to 0.5, as shown by the shaded area in Figure 6.

Regarding the threshold, different values were reported: 0.2 by both Han et al.[81] and Shivpuri et al.[35] in a case of 75°C impact; 0.1 by ElTobgy et al.[38] and Shivpuri et al.[35] in a case of perpendicular impact; and 0.25 by Meguid et al.[32] in a case of perpendicular impact. In another investigation, Ahmadi et al.[80] investigated the inhomogeneity of friction to plastic strain and reported that there was no threshold of friction to plastic strain while an optimum value was obtained at
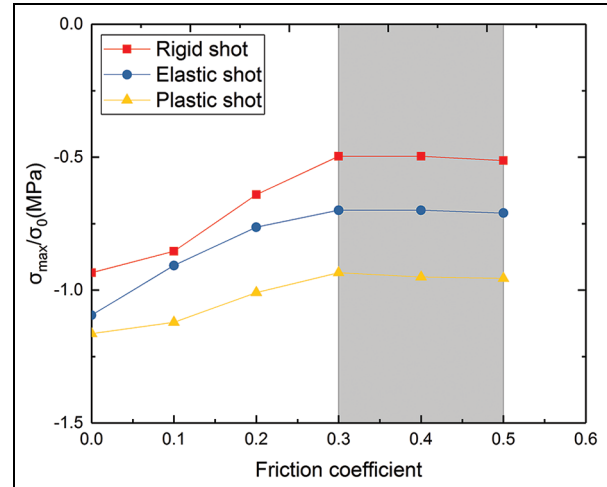

Figure 6. Variation of friction (μ) affecting stress profile for $\alpha = 45°$.
Adapted from Kim et al.[33]

$\mu = 0.5$. Below or above this optimum value, the change in friction coefficient could change the uniformity of distribution of plastic strain, while at this value, the plastic strain distributed most uniformly. Based on the threshold assumption, Shivpuri et al.[35] claimed that friction could not affect SP products since real friction coefficients were all higher than 0.1, which could be the threshold value according to their observation.

Some other investigators modified Coulomb's friction model with the argument that Coulomb's friction might be inappropriate to simulate the friction between the shot and the corresponding target surface. They consequently established their own customised friction model. Han et al.[81] and Meguid et al.[32] initially doubted the suitability of Coulomb's friction and subsequently proposed a modification to it which was done by Han et al.[81] by taking relative movement in the contact area prior to slip into consideration. This kind of slip was also considered by Sherafatnia et al.[82] when evaluating the effects of friction on residual stresses; and moreover, the mechanism of sliding was described in detail in this investigation. It was found that the effect of friction was dominant on the distribution of residual stresses in surface layers, and that the surface residual stresses decreased, while the maximum residual stresses increased partially as the coefficient of Coulomb's friction increased. A further systematic study is still missing on the modelling of friction and its effects on SP products.

Shot shape and material

It was reported that shot shape had effects on SP products,[27,83] although many investigations on SP simulation did not consider shot shape as an influential

parameter and hence used spherical shots.[26,49,78] However, an early investigation was conducted by Meguid et al.[84] who used steel ellipsoids with different aspect ratios as shots. Their work revealed that the compressed layer of material thickened as the aspect ratio of shot increased. Consistent results were observed yielding that the smaller the aspect ratio, the smaller the maximum surface residual stresses and smaller the surface roughness.[85] Consequently, the theory of elastic solid contacts proposed by Hertz[86] (see equation (3)) was used by Fathallah et al.[87] for determining the average contact pressure. This investigation related coefficient of restitution to shot shape and also deduced that the plastic deformation caused by cut-wire shots was not as large as that caused by spherical shots

$$P = \frac{R_0\left(R_1^{-1} + R_2^{-1}\right)}{E_1^{-1} + E_2^{-1}} \quad (3)$$

where P is the contact pressure; R_0, R_1 and R_2 are the radius of curvature of contact area, shot and plate, respectively; and E_1 and E_2 are the modulus of the two elastic solids.

Shots were also modelled with different material assumptions, that is, rigid,[29,41,44,49] elastic[55,78] and plastic[25,79] in different investigations. The topic attracted great attention from researchers who investigated the influence of shot material on the induced residual stresses and plastic strains where it was found that there was a threshold of hardness ratio of shot material to target material[88] as confirmed by ElTobgy et al.[38] The threshold ratio was 2 and when the ratio was less than this value, significant influence of shot hardness on SP products was reported while when it was greater than it no obvious influence was observed. Furthermore, many studies reported congruent results with this finding: rigid shots led to overestimation of residual stresses[32–34,38] as seen in Figure 6, where the stresses range from small to large when the shot material changes from plastic, to elastic to rigid. Another factor called a restitution coefficient was proposed and validated experimentally by Fathallah et al.[87] who comprehensively considered the influence of both shot hardness and shot shape. However, in industrial applications, shot materials usually had high hardness values compared to the corresponding target material[69] and large plastic deformation of shots were not acceptable.[32] Hence, the shots were usually modelled as rigid spheres.[44,89,90]

Coverage and intensity

Although coverage is one of the important parameters characterising reproducibility (including quality and effectiveness) of a SP[79,91–93] process and must be controlled,[94] there were discrepancies in coverage definition
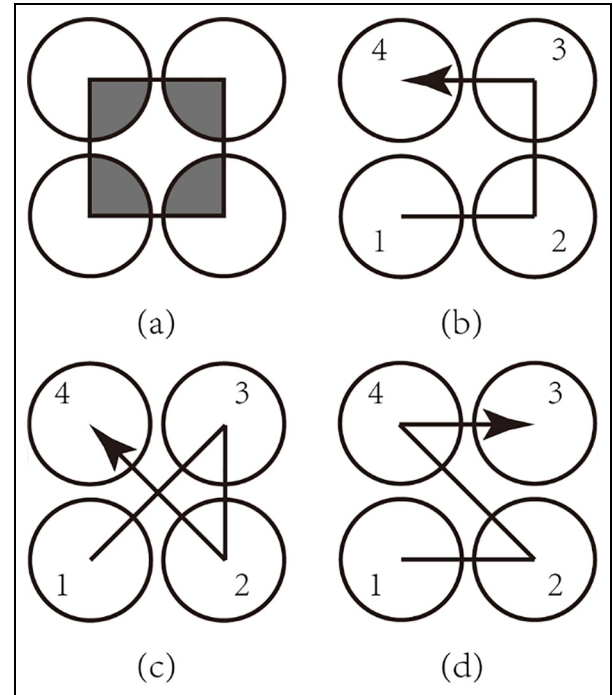
Figure 7. Coverage definition and the typical three arrangements of impacts: (a) definition of coverage which is the ratio of shading area to the rectangular area; and impact sequence in the order (b) 1-2-3-4, (c) 1-3-2-4 and (d) 1-2-4-3.

used by different researchers and hence, the arrangements of shot impact (or impact order) varied.

Some early investigations simply counted the number of impacts on the target surface so as to study the development of residual stresses, while coverage determination in such models was not applicable and consequently ignored.[52,95,96] It was observed in both simulation and experimental studies that subsequent impacts in the vicinity of the first impact area had influences on the surface residual stresses and the distribution of stresses beneath the surface. Hence, coverage was defined as a percentage of the peened surface (areas in plastic dents[16]) in relation to the whole target surface according to SAE J2277:2003,[97] as shown in Figure 7(a). Further investigations consistent with this coverage definition were carried out with distribution of impacts in various sequences on the target surface, as shown in Figure 7(b)–(d), so as to ideally determine the coverage and also avoid unnecessary computation cost.[34] It was found that both surface and maximum stresses increased as the centre distance of adjacent impact dents decreased. In contrast, other studies showed that impact sequence did not change the stress distribution but only the surface stress. These results are consistent with conclusions drawn by Baragetti.[98] In addition, Jianming et al.[99] found that the increase in coverage mainly improved the uniformity of residual

stress field in the compressed area. Interestingly, Zhan et al.[100] validated this conclusion experimentally. In terms of angle of impact, Miao et al.[27] studied the effect of impact angle on coverage, showing that a smaller angle resulted in larger coverage than peening the component at angle $\alpha = 90°$. A subsequent experimentally validated simulation study conducted by Kim et al.[79] derived three functions, which were the number of shots, coverage and shot velocity, respectively, for an arc height.

However, the above investigations neglected the flow behaviour of shots and randomness of impacts as in a real SP process, since these distributions of impacts are inherently exclusive with flow behaviour and randomness. Fortunately, the aforementioned FEM-DEMs have a promising potential to simulate these two characteristics of SP as they are more similar to industrial SP, its coverage is more related with time and is used together with intensity in the monitoring and control of SP.[3,93,101] Hence, in our viewpoint, the definition of coverage from SAE J2277:2003[97] applied in a FEM-DEM model could better predict the outputs of SP numerically.

Besides coverage, intensity is extremely important to the reproducibility of SP[93,94] and to explain real SP phenomena,[79] especially for controlled SP.[3,44] The method to measure intensity was innovatively introduced by Almen et al.[102] and the measured intensity is called Almen intensity. It was found that a higher intensity could be produced by either larger shot diameter or enhanced shot velocity; consequently, an increase in intensity resulted in an increase in the magnitude of depth of the maximum residual stresses.[91] Moreover, surface roughness could also increase with increasing Almen intensity.[103]

For the determination of saturation point of intensity, Karuppanan et al.[104] developed an algorithm by the means of a full regression analysis and fitted the experimental data by application of equation (4) which was also derived through data fitting by Miao et al.,[44] Jebahi et al.[21] and so on

$$h = \frac{A}{(T + B)^p} - \frac{A}{B^p} \tag{4}$$

where A, B and ρ are fitting parameters and T is the peening time. Another investigation for evaluating the saturation point was conducted by Rybakov[105] from an energy perspective. The author deduced the relationship between the bending energy required by saturation of the peened surface and the curvature of the craters induced by SP. This deduced relationship was proposed by the author to control the blasting operation with the use of a computer. It should be noted that the experimental data obtained to validate the deduced relationship deviated increasingly from the analytically

evaluated values as the peening time increased (see details from Rybakov[105]). Hence, the proposed method still requires more validations and improvements to resolve the potentially increasing deviations.

For numerically evaluating Almen intensity, Almen arc height h was related to residual stress profile through equation (5) by Guagliano[39] and related to impact number N by Miao et al.[44] using equation (6). These two equations were derived through fitting simulation results derived by other researchers such as Miao[89] and Tu et al.[106] Other equations to predict arc height of intensity through either coverage or number were derived by Kim et al.[79] based on an area-averaged solution. Encouragingly, results predicted by the two equations corresponded well with the experimental results obtained from Kim et al.[24,34] The latest progress in this aspect is the prediction function for Almen height which was derived through the regression method.[107] This function revealed that peening time, shot diameter, air pressure and their combinations had significant effects on Almen intensity

$$h = \frac{3Ml^2}{2Ebt^3} \tag{5}$$

$$h = \frac{p_1 N^2 + p_2 N}{N + p_3} \tag{6}$$

where E is Young's modulus of strip; l, b and t are, respectively, its length, width and thickness; M is the moment induced by residual stress; and p_1, p_2 and p_3 are the fitting parameters.

Numerical evaluation of residual stress and strain hardening

In terms of evaluation of residual stresses, the review found that the single-node average method was used widely by researchers such as Schiffner and Droste gen. Helling,[4] Han et al.[81] and Boyce et al.[59] at the early stage of finite element analyses. Then, node-average method was applied as attempts to obtain more accurate residual stresses. This method evaluates the residual stresses of the impact centre by averaging the stresses at the surrounding nodes. Four nodes involved in the averaging is called four-node-averaged method and nine nodes involved is called nine-node-averaged method.[34] Subsequently, this method was modified by expanding from averaging a portion of nodes to averaging all the surrounding nodes. This expanded method is called area-averaged method.[79] Finite element results obtained through the area-averaged method were reported to have better correlation with experimental data obtained through the X-ray diffraction method[34] since the X-ray diffraction method is also an 'area-averaged[79,108] method.

Notably, material hardening is a favourable product of SP which directly enhances the hardness of the target material[4,72,109] by increasing the yield stress of the material.[5,110] Material hardening occurs due to the dislocations within the crystals of the material.[5,111] The comprehensive process of the formation of these dislocations is nicely detailed by Kirk[111] where it was reported that material hardening was affected by several parameters of SP, such as intensity[5] and peening time.[112] However, it is easily mistaken that increasing these parameters would strengthen the effect of strain hardening, which is not true as the hardening is annihilated when the plastic strain reaches a certain value and a larger strain will just induce material softening.[72] For this reason, it is important to assess the contribution of strain hardening induced in the target material or evaluate the beneficial effects of strain hardening. The direct approach to evaluating strain hardening is to evaluate the hardness of the peened and unpeened materials, respectively. The method for evaluating Brinell's hardness recommended by Kirk[113] is expressed in equation (7)

$$H_B = \frac{P}{(\pi D/2)\left(D - (D^2 - d^2)^{0.5}\right)} \qquad (7)$$

where H_B is Brinell's hardness, P is the applied force, and D and d are the diameter of the ball and of the indentation it induced, respectively.

However, assessment of the effects of strain hardening is complex. Since strain hardening improves the fatigue life of the material, one method could be identifying the difference between the S-N curves of peened and unpeened materials.[111] The disadvantage of this method is that it cannot differentiate the effect of strain hardening from the improved fatigue life of the peened material which is the complimentary effect of strain hardening and CRSs. The other method proposed by Kirk[111] is used to separate the effects of the two contributors, namely, strain hardening and CRS. This method realises the assessment of the respective contributions of strain hardening and CRS pictorially through comparisons between the two Goodman lines of the unpeened material without alternating stresses and peened material with alternating stresses. The corresponding cross-hatched area of the two Goodman lines represents the contribution of strain hardening.

It can be said that the above methods do successfully characterise the effects of strain hardening on a material, depending from which perspective it is analysed. Furthermore, the evaluation of hardness is a direct and quantitative way to depict the effect of strain hardening on a material, and the other two methods reflect the effect of both through the improved fatigue life of the
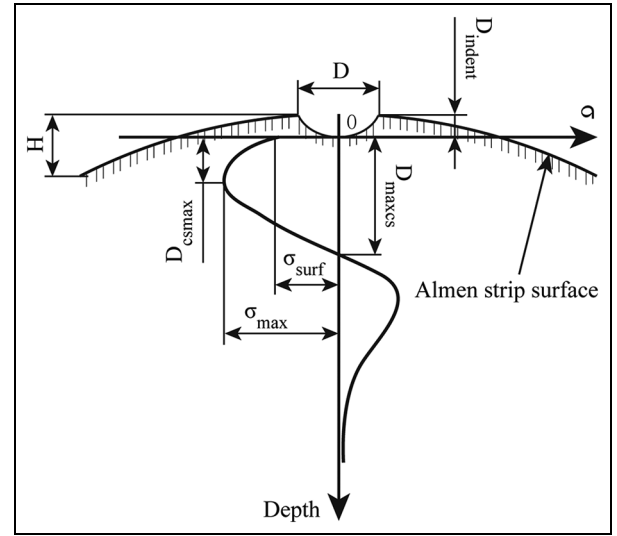

Figure 8. Schematic diagram of responses relevant to optimisation objective.
σ_{surf} is the surface residual stress, σ_{max} is the maximum CRS, D_{csmax} is the distance of σ_{max} to target surface, D_{maxcs} is the maximum depth of compressive layer, D is the diameter of indent induced by impacts, D_{indent} is the depth of the indent and H is the Almen arc height.

material with the differences being that one is done via S-N curves, while the other is assessed through Goodman lines.

Numerical optimisation

Objective functions

As shown in Figure 2, SP is affected by many factors and mainly has three products, namely, residual stresses, surface roughness and cold work. In optimisation studies, different investigations considered different factors and responses due to limited physical conditions or specific purposes. Some responses were simplified by emphasis on some aspects of their corresponding responses. For example, residual stresses refer to many aspects, namely, surface residual stress, maximum residual stress and distribution of residual stresses, but the objective might be just set as some of these aspects rather than all of them. In order to illustrate these variables, a Cartesian coordinate system is defined with residual stress as its abscissa (labelled σ) and distance from the target surface as its ordinate (labelled depth), as shown in Figure 8.

The variables (products of SP) in Figure 8 can be divided into three kinds, namely, residual stress, cold work and surface roughness. Residual stresses on the top layer are beneficial to enhance the fatigue resistance of the target material, hence it should be maximised. Nevertheless, the cold work may lead to stress

relaxation of CRS on one hand,[11] and on the other hand, surface roughness in terms of the height of the cavities caused by impacts which have the potential to weaken the benefits of CRSs by causing corrosive cracks[83] and stress concentrations.[11] Thus, these two products are unfavourable in industrial applications and thus should be controlled to acceptable levels. Furthermore, these SP products are measurable: the residual stresses could be evaluated by several methods, such as the area-averaged method as aforementioned; the cold work can be calculated by measuring the material plastic strain at the yield point of the target material; and the surface roughness can be calculated by measuring the plastic strain of the peened surface.[45] Therefore, with the consideration of both SP effects on target material and measurability (quantification) of these effects, applicable objectives of the SP optimisation should be as follows: (1) maximisation of the CRSs, (2) minimisation of cold work and (3) minimisation of surface roughness.

Maximisation of residual stress. Induction of compressed residual stresses to enhance fatigue life of components is the initial purpose of utilisation of SP surface treatment; hence, maximisation of residual stresses (such as σ_{surf} and σ_{max}) and their corresponding indicators of compressed depth (such as D_{csmax} and D_{maxcs}) was an objective in optimisations of SP in early investigations. It is ideal to maximise all of these responses; nevertheless, the object was usually set as maximisation of the maximum residual stresses along the depth of target material at the impact centre, while the other responses were set as constraints to control them to acceptable levels. For example, all the responses, σ_{max}, σ_{surf}, D_{csmax} and D_{maxcs}, together with some other responses were set as objectives at the same time in the early investigation by Baragetti[1] for their optimisation of SP, while many later investigations just set σ_{max} as objective function, such as investigations conducted by Romero et al.,[109] Levers et al.,[114] Petit-Renaud et al.[115] and Baskaran et al.,[11] and set the other responses (such as σ_{surf}) as constraints.[115]

Minimisation of surface roughness. The surface roughness relevant responses, namely, D_{indent} and D, are to be minimised and this was obtained by setting surface roughness as an objective in some of the studies[11,103,107] mentioned here. Some early studies additionally considered D and D_{indent} simultaneously, such as the work done by Baragetti,[1] while surface roughness definitions were later introduced and essentially expressed via a surface roughness, R_a, which is a ratio of the total height of peaks, D_{indent}, on the peened surface to the corresponding measured length, L, as shown in equation (8)

$$R_a = \frac{1}{L} \sum_{i=1}^{N} D_{indent} \qquad (8)$$

Minimisation of cold work. Cold work is another response to be minimised which was set as a minimisation sub-objective function of optimisation in the investigations conducted by Levers et al.,[114] Romero et al.[109] and Baskaran et al.,[11] where it was defined as the amount of true plastic strain producing the observed diffraction peak broadening[116] and was expressed as a function of material strain parameters,[45] as described in equation (9)

$$CW = \frac{\sigma_{ref}}{\sigma_{0.2}} \times 100 = \left(\frac{\varepsilon_{ref}}{\varepsilon_{0.2}}\right)^n \times 100 \qquad (9)$$

where ε_{ref} is the plastic strain through-plate-thickness, $\varepsilon_{0.2}$ is the strain at yield point and n is the material-hardening exponent.

Other objectives. Besides the above three frequently used objectives, some other responses were also used as optimisation objectives, such as fatigue life,[109] coverage,[117] Almen height (H)/intensity of target component[6,107,117] and difference between the desired deformation and the real deformation.[118] Coverage and intensity are basically two control parameters and are recommended by the authors of this work to be constraints rather than objectives. It should be noted that material hardening unfortunately has not been specified as an objective function although it actually has a very significant effect induced by SP.[72]

Tackling method with multiple objectives. It can be seen that the optimisation is a multi-objective problem and the sub-objectives may conflict with each other so that they cannot be optimised simultaneously. Furthermore, most multi-objective problems just have several feasible solutions rather than only one optimum solution. A popular method called the *weighted-sum*[119] may produce different optimum solutions led by the alternative weights. Another popular method is *ε -constraints*[119] method which designates a sub-objective as the primary objective while constraining the others. This method can only apply to those sub-objectives whose right-hand side constraints are certain but not suitable for those with uncertain constraints. However, Pareto optimality can obtain combinations of the multi-objective function and provides flexibility to engineers to choose an optimum solution from the obtained combinations.[120] Hence, deciding on what method to use mainly depends on the purpose of the investigation. Affirmatively, the weighted-sum method could be desirable when the weights of sub-objectives are specific, while Pareto

optimality could be used when addressing a general optimality problem.

Design constraints

For optimisation purposes, only influential and also controllable parameters were taken into account in the reviewed literature and are summarised in this work. These parameters include the initial velocity, diameter of the shot, incidence angle, exposure time, material of shot and target, and coverage. Each parameter here has its own range which is discussed as follows.

First, the initial velocity could be specified from 20 to 100 m/s according to Frija et al.,[15] while Marsh[121] set it as 40 to 120 m/s. Although Soady[3] contended that it ranged from 40 to 70 m/s, the range from 20 to 120 m/s could safely cover the whole range from an industrial perspective. Second, the size/diameter of shots should be discrete values between 0.0450 and 4.75 mm[122] and the values are specified in SAE.[122] Note that most researchers[123] specified the values according to this range, while 38 mm was used in a 3D model by Klemenz et al.[48] for the purpose of easy validation with a physical experiment. However, it should be noted that such a large shot was developed specifically for the purpose of easy validation with physical experiments but should not be advocated. Third, values of the incidence angle could be specified at a range of 45°–90° with respect to the target surface[33] since this range has no controversy and is economical in terms of the utilisation of the shots' kinetic energy. However, values ranging from 0° to 45° was also used by Shivpuri et al.[35] where it was demonstrated that incidence angle at this range has a feeble effect on SP results.[33] Fourth, pre-stressing conditions for SP could be set as pre-stressed or not, since pre-stressing techniques could increase the maximum CRS.[124] Fifth, the exposure time could be simplified as the peening time on the surface since the longer the exposure time, the larger is the probabilistic peening time of the surface. Sixth, the material of shots could be specified as the commonly used materials, namely, ceramic, steel and glass, according to Champaigne[125] and Frija et al.[15] Finally, the target material should be specified according to what kind of component a researcher is studying since different components have different material compositions.

Interestingly, in some investigations, intensity and coverage were also set as constraints. Coverage was taken as a constraint with two levels (one impact or two at the impingement centre) by Baragetti[1] who concluded that percentage of coverage could be one of the most important factors affecting residual stress field. Subsequently, both coverage and intensity were constrained by Romero et al.[109] and Vielma et al.,[103] who derived the same conclusion that coverage could be one of the most influential factors affecting the profile of residual stresses. Some other variables were also set as constraints, such as peening duration (exposure time),[12,107,115,117] mass flow rate,[115] nozzle distance,[12,117] air pressure,[12,103,107,115,117,126] friction[11] and interaction effects,[107,115] among these variables. Note that some of these factors have relationships more or less to factors mentioned above. For example, air pressure is highly related to shot velocity yet they emanate from different models, that is, shot velocity from 3D finite element models while air pressure from particle models.

Tools and models for SP

There are mainly two kinds of models used in SP optimisation, namely, finite element models and approximation models. The latter models work as approximations/surrogates of the input/output function. They are formulated based on the fundamental input/output data produced by numerical simulation or physical experimentation through some specific methods,[127] such as response surface method and polynomial fitting methods.

Early investigations conducted developed finite element models directly for the optimisation of SP. An interesting 3D finite element model for optimisation was created by Baragetti[1] with 100% coverage (single-shot impact) and 200% coverage (two-shot impact at the same location) in Abaqus explicit code. Four inputs, including shot diameter, shot velocity, plate material and coverage, were set for this model and only two levels for each input. Another important model combining finite elements with discrete elements was created by Miao et al.[27] in Abaqus code synthesising with an EDEM code. The model considered flow rate and coefficient of restitution first in optimisation model and also took interactions between shots into account. Although the model focused on optimisation of CRSs, it did not consider surface roughness which is detrimental to material fatigue life.

However, approximation models are usually established on the basis of simple finite element analyses or physical experimental results through different methods such as radial basis function (RBF), response surface methodology and polynomial function. By the utilisation of RBF, Baskaran et al.[11] created an approximation model in PEZ software with shot radius, incidence angle and shot velocity as inputs and CRS, cold work and surface roughness as outputs, respectively. They compared the prediction precisions among the polynomial model, RBF model and the finite element model and concluded that the RBFs had the highest prediction precision covering all sampling points, which is favourable for optimisation. The response surface method was applied through a polynomial function (equation (10))

in Minitab code[107,115] and Design-Expert code[117] for establishing surface responses, respectively, for outputs in relation to inputs. The outputs include residual stresses, surface roughness, arc height, surface hardness, coverage and intensity, and the inputs include nozzle size, nozzle distance, pressure, flow rate, angle and exposure time. The models established through this equation were capable of studying interactions between design variables through the crossing item, $x_i x_j$, and they obtained relatively reliable precisions

$$Y = b_0 + \sum b_i x_i + \sum b_{ii} x_i^2 + \sum b_{ij} x_i x_j + e_r \quad (10)$$

where Y is the surface response; b_0 is a constant; x_i and x_j are the input parameters; and b_i, b_{ii} and b_{ij} are the linear, quadratic and interaction coefficients, respectively.

Other models were also used in SP optimisation studies such as an analytical model which was created by Hu et al.[118] based on an assumed relationship between arc height and exposure time in MATLAB code. It used a notional temperature gradient to approximate macroscopic deformation and only took plastic deformation into account. However, this model over-simplified the SP process drastically that it could not even evaluate CRSs.

Optimisation algorithms

Design of experiments methods. Many studies on SP optimisation have been done using different optimisation methods so far among which the most commonly used method is the design of experiments (DOE). An early important investigation done by Baragetti[1] using Taguchi's method to analyse the numerical simulation results of SP resulted in the optimisation of seven parameters. Later, Evans[110] derived mathematical expressions for the indentation of surfaces and proposed a plausible procedure for the optimisation of SP. Rodopoulos et al.[17] used the effects neutralisation model, apart from the DOE, to optimise the parameters of SP and efforts were made to define the optimum levels and tolerances. One of their important initiatives was the stress relaxation that was employed to examine the stability of CRSs. Nevertheless, there were only two levels setting to each parameter specified. George et al.[6] used Taguchi's method to optimise process parameters of SP with two levels of each design variable from the selected four parameters and analysed interactions between the parameters. However, the shortfall of these investigations comprises the following: (a) symmetric BCs were used which lead to imbalance of in-depth residual stress profile according to Klemenz et al.[41,53]; (b) the rigid shot assumption may increase the amplitude of CRSs; (c) the optimisation objective is only the CRSs; and (d) most importantly, the setting of only two levels for each parameter

affects reliability of the results.[1] Unfortunately, all these investigations using the DOE method limited their design variables to two levels, which led to loss of fidelity of the results to some extent. The reason may be that an increase in level number would increase the number of iterations required for a solution and thereby increase computational cost.

Other algorithms. Besides the DOE, other methods were also used for optimisation of SP. Baragetti et al.[128] proposed a numerical procedure which could predict SP effects through a non-dimensional function. With this numerical procedure, it is possible to choose SP parameters for a particular application. Petit-Renaud et al.[115] established an empirical relationship between input variables, such as exposure time and nozzle size, and response variables (residual stresses and their corresponding distance to the target surface); and based on this relationship, they optimised the process parameters. Miao et al.[5] independently considered the surface integrity as the optimisation objective to optimise a SP process. Later, using genetic algorithm, Baskaran et al.[11] set the increase in residual compressive stress, reduction in surface roughness and cold work as objectives of an optimisation function and achieved an optimised set of parameters. This was a multi-objective optimisation which first considered friction between the shot and its corresponding surface. This investigation resulted in the determination of the optimum area under the CRS curve while keeping the cold work and surface roughness under the specification limits. Recently, the Box–Behnken design (BBD) method was used by Nam et al.[117] who set the Almen height as the objective of a desirability function and claimed that BBD provided high-quality predictions in investigations on linear, quadratic and interaction effects of parameters.

Critical analysis of the optimisation algorithms. Among these investigations, Baragetti et al.[128] developed a software package for the prediction of compressive residual, and Petit-Renaud et al.[115] used a non-orthogonal experimental design and fitted multiple regressions to the results. The disadvantage of these investigations is that these researchers just regarded the SP as a single objective problem which does not correspond to a real SP process. Miao et al.[5] did not optimise the SP process while their investigation on the relationship between parameters and the responses, namely, residual stresses and surface roughness, is very important for further optimisation work. The wide application of the DOE algorithm could perhaps be due to it not requiring highly skilled staff and is cost-saving, efficient and capable of taking interactions between variables into consideration. However, it is not applicable when the

range of variables is wide and the variables are continuous. Nearly all the investigations with DOE aforementioned did not consider more than three levels of each variable. BBD and other similar algorithms have similar disadvantages to DOE. Contrarily, some recently developed modern algorithms, such as the genetic algorithm, displayed promising results for searching optimal combinations of parameters. In this regard, Baskaran et al.[11] conducted a very comprehensive investigation on the optimisation of SP, However, its drawback was that the study did not consider the independence test of those influential parameters before optimisation and material hardening was also not considered.

Summary and discussions

This article comprehensively reviewed the definition, influential parameters, responses and different aspects of numerical simulation and optimisation of SP found in the existing literature in recent years. The work reviewed is summarised and concluded as follows.

Regarding the simulation of SP, 3D models are currently the mainstream since they are capable of considering coverage and predicting the distribution of residual stresses more precisely. The FEM-DEMs, however, are becoming increasingly mature and show their advantages in incorporating flow behaviour and randomness of shots. More attention is expected to be paid to this type of models in future. The SP process can be simulated through two analysis steps, that is, combining a dynamic step with a sequential static step. High emphasis was paid on the material modelling of target material since it is the key factor influencing the responses of simulation models of SP. SRS, cyclic behaviour and Bauschinger effects are recommended to be taken into account simultaneously since considering only one of them may lead to unreliable residual stress distributions. In general, the target materials in SP are strain-rate sensitive in most cases and always undergo cyclic loadings. Therefore, it is appropriate to apply an elastic–viscous–plastic combined hardening material model when taking all these factors into account. Thermal effects are expected to be incorporated when thermal loadings are capable of causing stress relaxation though it does not reach such severity in most cases. Friction between shots and a target material is expected to be systematically studied in future works. The most prevailing shot shape is a spherical solid and the material is usually set as rigid although the shape and material are reported to having influences on the distribution of residual stresses. There are discrepancies in the definition of coverage and intensity though they are two critical controllable factors characterising the reproducibility of a SP process and the standard definitions from SAE are highly recommended for them. The

area-averaged method for numerically evaluating residual stresses is currently reported to produce the most accurate results. Different methods are available for the characterisation of strain hardening though their reliability needs to be assessed in context accordingly. The review also showed that material hardening is one of the important benefits of a SP process although it has not received its deserved attention.

In terms of numerical optimisation, the prevailing objective function is the distribution of residual stresses though cold work and surface roughness also received a certain extent of concern. In essence, cold work is highly related to surface roughness which can be readily seen from their definitions. Material hardening, more specifically the hardness enhancement, has not been set as an objective function so far although it is as beneficial as residual stresses. The coverage and intensity of SP are commonly excluded in most optimisation research though they are critical control parameters. The influential parameters recommended as design constraints are initial velocity, diameter of the shot, incidence angle, exposure time, material of shot and target, coverage and intensity. SAE has some standards specifying the ranges of these parameters. The main models applied in optimisation are the finite element and approximation models. DOE is the most widely applied algorithm because of its advantages. However, it is not applicable when the range of variables is wide and the variables are continuous. Nearly all investigations with DOE aforementioned did not consider more than three levels of each variable. On the contrary, some recently developed heuristic algorithms, such as the genetic algorithm, showed promise in searching for optimal combinations of parameters. It can be easily seen that approximation models based on finite element simulation models have obvious advantages in terms of computational costs. The models used in simulation are generally different from those in optimisation. The reason might be that SP models for optimisation are required to be as simple as possible in order to avoid high computational times arising from numerous iterations. However, it can be expected that these algorithms, blending with approximation models, are to attract more attention of future researchers.

Declaration of conflicting interests

The author(s) declared no potential conflicts of interest with respect to the research, authorship and/or publication of this article.

ORCID iD

Jun S Chen https://orcid.org/0000-0001-8847-3766

References

1. Baragetti S. Shot peening optimisation by means of DOE: numerical simulation and choice of treatment parameters. *Int J Mater Prod Tec* 1997; 12: 83–108.
2. James MN, Newby M, Hattingh DG, et al. Shot-peening of steam turbine blades: residual stresses and their modification by fatigue cycling. *Proced Eng* 2010; 2: 441–451.
3. Soady KA. Life assessment methodologies incorporating shot peening process effects: mechanistic consideration of residual stresses and strain hardening part 1 – effect of shot peening on fatigue resistance. *Mater Sci Tech* 2013; 29: 637–651.
4. Schiffner K and Droste gen. Helling C. Simulation of residual stresses by shot peening. *Comput Struct* 1999; 72: 329–340.
5. Miao H, Zuo DW, Wang HF, et al. Effect of optimization of shot peening parameters on surface integrity of NAK80. In: Zuo DW, Guo H, Tang GX, et al. (eds) *Functional manufacturing technologies and Ceeusro I.* Changzhou, PR CHINA: Trans Tech, 2010, pp.537–539.
6. George PM, Pillai N and Shah N. Optimization of shot peening parameters using Taguchi technique. *J Mater Process Tech* 2004; 153: 925–930.
7. Kirk D. Shot peening. *Aircr Eng Aerosp Tec* 1999; 71: 349–361.
8. Sanjurjo P, Rodriguez C, Penuelas I, et al. Influence of the target material constitutive model on the numerical simulation of a shot peening process. *Surf Coating Tech* 2014; 258: 822–831.
9. Purohit R, Verma CS, Rana RS, et al. Optimization of process parameters of shot peening using ABQUS. *Mater Today: Proc* 2017; 4: 2119–2128.
10. Hong T, Ooi JY and Shaw B. A numerical simulation to relate the shot peening parameters to the induced residual stresses. *Eng Fail Anal* 2008; 15: 1097–1110.
11. Baskaran B, Srinivasan SM, Bob M, et al. Constrained probabilistic multi-objective optimization of shot peening process. *Eng Optimiz* 2011; 43: 657–673.
12. Yildiran Y, Avcu E and Sinmazçelik T. Optimization of surface properties of shot peened Ti6Al4V alloy. *Acta Phys Pol A* 2015; 127: 984–986.
13. Waterhouse RB. Residual stresses and fretting, crack initiation and propagation. *Adv Surf Treat Technol* 1987; 4: 511–525.
14. Burmeister TJ. Peen forming of airfoil shapes for aircraft wing sections. In: Fuchs H (ed.) *Proceedings of the second international conference on shot peening.* Paramus, NJ: American Shot Peening Society, 1984, pp.1–5.
15. Frija M, Hassine T, Fathallah R, et al. Finite element modelling of shot peening process: prediction of the compressive residual stresses, the plastic deformations and the surface integrity. *Mat Sci Eng A: Struct* 2006; 426: 173–180.
16. Kirk D. Peening impressions (Dents). *Shot Peen* 2013; 27: 24–32.
17. Rodopoulos CA, Curtis SA, de los Rios ER, et al. Optimisation of the fatigue resistance of 2024-T351 aluminium alloys by controlled shot peening – methodology, results and analysis. *Int J Fatigue* 2004; 26: 849–856.
18. Calle MAG and Alves M. Multibody modeling of the shot peening process. *J Braz Soc Mech Sci* 2014; 36: 111–124.
19. Bhuvaraghan B, Srinivasan SM, Maffeo B, et al. Shot peening simulation using discrete and finite element methods. *Adv Eng Softw* 2010; 41: 1266–1276.
20. Bagherifard S, Ghelichi R and Guagliano M. On the shot peening surface coverage and its assessment by means of finite element simulation: a critical review and some original developments. *Appl Surf Sci* 2012; 259: 186–194.
21. Jebahi M, Gakwaya A, Lévesque J, et al. Robust methodology to simulate real shot peening process using discrete-continuum coupling method. *Int J Mech Sci* 2016; 107: 21–33.
22. Zimmermann M and Klemenz M. Literature review on shot peening simulation. *Int J Comput Mater Sci Surf Eng* 2010; 3: 289–310.
23. Kang X, Wang T and Platts J. Multiple impact modelling for shot peening and peen forming. *Proc IMechE, Part B: J Engineering Manufacture* 2010; 224: 689–697.
24. Kim T, Lee H, Hyun HC, et al. A simple but effective FE model with plastic shot for evaluation of peening residual stress and its experimental validation. *Mat Sci Eng A: Struct* 2011; 528: 5945–5954.
25. Hassani-Gangaraj SM, Cho KS, Voigt HJL, et al. Experimental assessment and simulation of surface nanocrystallization by severe shot peening. *Acta Mater* 2015; 97: 105–115.
26. Romero-Angeles B, Urriolagoitia-Sosa G, Miguel CRT-S, et al. Numerical simulation of the shot peening process under previous loading conditions. *J Phys Conf* 2015; 582: 012004.
27. Miao HY, Larose S, Perron C, et al. Numerical simulation of the stress peen forming process and experimental validation. *Adv Eng Software* 2011; 42: 963–75.
28. Hong T, Wen DH and Yuan JL. Optimising shot peening parameters using finite element and discrete element analysis. *Appl Mech Mater* 2008; 10–12: 493–497.
29. Edward AB, Heyns PS and Pietra F. Shot peening modeling and simulation for RCS assessment. *Procedia Manuf* 2016; 7: 172–177.
30. Dassault Systèmes. *Abaqus analysis user's guide.* Providence, RI: Dassault Systèmes, 2016.
31. Kim T, Lee H, Kim M, et al. A 3D FE model for evaluation of peening residual stress under angled multi-shot impacts. *Surface & Coatings Technology* 2012; 206: 3981–3988.

32. Meguid SA, Shagal G and Stranart JC. 3D FE analysis of peening of strain-rate sensitive materials using multiple impingement model. *Int J Impact Eng* 2002; 27: 119–134.

33. Kim T, Lee H, Hong CH, et al. Effects of Rayleigh damping, friction and rate-dependency on 3D residual stress simulation of angled shot peening. *Mater Design* 2013; 46: 26–37.

34. Kim T, Lee H, Jung S, et al. A 3D FE model with plastic shot for evaluation of equi-biaxial peening residual stress due to multi-impacts. *Surf Coat Tech* 2012; 206: 3125–3136.

35. Shivpuri R, Cheng XM and Mao YN. Elasto-plastic pseudo-dynamic numerical model for the design of shot peening process parameters. *Mater Design* 2009; 30: 3112–3120.

36. Sun J and Zhang Y. Three-Dimensional Finite Element Simulation of Residual Stress Field For Shot-Peening and Grinding. In: *Proceedings of the International Conference on Electromechanical Control Technology and Transportation* (eds YH Shyu and Y Zhang), 2015, pp. 382–386.

37. Majzoobi GH, Azizi R and Nia AA. A three-dimensional simulation of shot peening process using multiple shot impacts. *J Mater Process Tech* 2005; 164: 1226–1234.

38. ElTobgy MS, Ng E and Elbestawi MA. Three-dimensional elastoplastic finite element model for residual stresses in the shot peening process. *Proc IMechE, Part B: J Engineering Manufacture* 2004; 218: 1471–1481.

39. Guagliano M. Relating Almen intensity to residual stresses induced by shot peening: a numerical approach. *J Mater Process Tech* 2001; 110: 277–286.

40. Yang C, Hodgson PD, Liu Q, et al. Geometrical effects on residual stresses in 7050-T7451 aluminum alloy rods subject to laser shock peening. *J Mater Process Tech* 2008; 201: 303–309.

41. Klemenz M, Zimmermann M, Schulze V, et al. Numerical prediction of the residual stress state after shot peening. In: Nagel WE, Jäger W and Resch M (eds) *High performance computing in science and engineering*. Berlin: Springer-Verlag, 2007, pp.437–448.

42. Gariepy A, Larose S, Perron C, et al. Shot peening and peen forming finite element modelling – towards a quantitative method. *Int J Solids Struct* 2011; 48: 2859–2877.

43. Amarchinta HK, Grandhi RV, Clauer AH, et al. Simulation of residual stress induced by a laser peening process through inverse optimization of material models. *J Mater Process Tech* 2010; 210: 1997–2006.

44. Miao HY, Larose S, Perron C, et al. On the potential applications of a 3D random finite element model for the simulation of shot peening. *Adv Eng Softw* 2009; 40: 1023–1038.

45. Mylonas GI and Labeas G. Numerical modelling of shot peening process and corresponding products: residual stress, surface roughness and cold work prediction. *Surf Coat Tech* 2011; 205: 4480–4494.

46. Bagherifard S, Ghelichi R and Guagliano M. Numerical and experimental analysis of surface roughness generated by shot peening. *Appl Surf Sci* 2012; 258: 6831–6840.

47. Mahmoudi AH, Ghasemi A, Farrahi GH, et al. A comprehensive experimental and numerical study on redistribution of residual stresses by shot peening. *Mater Design* 2016; 90: 478–487.

48. Klemenz M, Schulze V, Rohr I, et al. Application of the FEM for the prediction of the surface layer characteristics after shot peening. *J Mater Process Tech* 2009; 209: 4093–4102.

49. Mann P, Miao HY, Gariepy A, et al. Residual stress near single shot peening impingements determined by nanoindentation and numerical simulations. *J Mater Sci* 2015; 50: 2284–2297.

50. Dassault Systèmes. *Abaqus/CAE user's guide*. Providence, RI: Dassault Systèmes, 2016.

51. Campbell JD and Ferguson WG. The temperature and strain-rate dependence of the shear strength of mild steel. *Philos Mag* 1970; 21: 63–82.

52. Kobayashi M, Matsui T and Murakami Y. Mechanism of creation of compressive residual stress by shot peening. *Int J Fatigue* 1998; 20: 351–357.

53. Klemenz M, Schulze V, Vohringer O, et al. Finite element simulation of the residual stress states after shot peening. *Mater Sci Forum* 2006; 524–525: 349–354.

54. Al-Hassani STS, Kormi K and Webb DC. Numerical simulation of multiple shot impact. In: *The 7th international conference on shot peening* (ed A Nakonieczny), Warsaw, 28 September–1 October 1999, pp.217–227. Mishawaka: Electronics Inc.

55. Bagherifard S, Ghelichi R and Guagliano M. A numerical model of severe shot peening (SSP) to predict the generation of a nanostructured surface layer of material. *Surf Coat Tech* 2010; 204: 4081–4090.

56. Yang F, Chen Z and Meguid SA. Effect of initial surface finish on effectiveness of shot peening treatment using enhanced periodic cell model. *Int J Mech Mater Des* 2015; 11: 463–478.

57. Bhuvaraghan B, Srinivasan SM and Maffeo B. Numerical simulation of Almen strip response due to random impacts with strain-rate effects. *Int J Mech Sci* 2011; 53: 417–424.

58. Cowper GR and Symonds PS. Strain hardening and strain rate effect in the impact loading of cantilever beams. *SBE* 1957; 31: 235–263.

59. Boyce BL, Chen X, Hutchinson JW, et al. The residual stress state due to a spherical hard-body impact. *Mech Mater* 2001; 33: 441–454.

60. Calle Gonzales MA, Barrios DB, de Lima NB, et al. Importance of considering a material micro-failure criterion in the numerical modelling of the shot peening process applied to parabolic leaf springs. *Lat Am J Solid Struct* 2010; 7: 21–40.

61. Ekström K. *Experimental investigation of the strain rate dependence of SS2506 gear steel*. Stockholm: KTH Royal Institute of Technology, 2013.

62. Kim T, Lee H, Kim M, et al. A 3D FE model for evaluation of peening residual stress under angled multi-shot impacts. *Surf Coat Tech* 2012; 206: 3981–3988.

63. Johnson GR and Cook WH. A constitutive model and data for metals subjected to large strains, high strain rates and high temperatures. In: *Proceedings of the seventh international symposium on ballistics*, The Hague, 19–21 April 1983, pp.541–547.

64. Salahi AAA and Othman R. Constitutive equations of yield stress sensitivity to strain rate of metals: a comparative study. *J Eng* 2016; 2016: 3279047.

65. Martin U, Altenberger I, Scholtes B, et al. Cyclic deformation and near surface microstructures of normalized shot peened steel SAE 1045. *Mat Sci Eng A: Struct* 1998; 246: 69–80.

66. Altenberger I, Scholtes B, Martin U, et al. Cyclic deformation and near surface microstructures of shot peened or deep rolled austenitic stainless steel AISI 304. *Mat Sci Eng A: Struct* 1999; 264: 1–16.

67. Zimmermann M, Klemenz M, Schulze V, et al. Numerical studies on the influence of thickness on the residual stress development during shot peening. In: Nagel WE, Kröner DB and Resch MM (eds) *High performance computing in science and engineering*. Berlin: Springer-Verlag, 2009, pp.481–492.

68. Rouhaud E, Ouakka A, Ould C, et al. Finite elements model of shot peening, effects of constitutive laws of the material. In: *Proceedings of the 9th international conference on shot peening (ICSP-9)*, Paris, 6–9 September 2005. Amsterdam: Elsevier.

69. Meguid SA, Shagal G, Stranart JC, et al. Relaxation of peening residual stresses due to cyclic thermo-mechanical overload. *J Eng Mater: T ASME* 2005; 127: 170–178.

70. Urriolagoitia-Sosa G, Durodola JF and Fellows NA. Determination of residual stress in beams under Bauschinger effect using surface strain measurements. *Strain* 2010; 39: 177–185.

71. Bannantine J. *Fundamentals of metal fatigue analysis*. Upper Saddle River, NJ: Prentice Hall, 1989.

72. Kirk D. Review of shot peened surface properties. *Shot Peen* 2007; 21: 24–30.

73. Harada Y and Mori K. Effect of processing temperature on warm shot peening of spring steel. *J Mater Process Tech* 2005; 162–163: 498–503.

74. Kirk D. Surface heating caused by peening. *Shot Peen* 2003; 17: 18–20.

75. Rouquette S, Rouhaud E, François M, et al. Coupled thermo-mechanical simulations of shot impacts: effects of the temperature on the residual stress field due to shot-peening. *J Mater Process Tech* 2009; 209: 3879–3886.

76. Hu D, Gao Y, Meng F, et al. A unifying approach in simulating the shot peening process using a 3D random representative volume finite element model. *Chinese J Aeronaut* 2017; 30: 1592–1602.

77. Kocks UF, Argon AS and Ashby MF. Thermodynamics and kinetics of slip. *Prog Mater Sci* 1975; 19: 171–229.

78. Gangaraj SMH, Guagliano M and Farrahi GH. An approach to relate shot peening finite element simulation to the actual coverage. *Surf Coat Tech* 2014; 243: 39–45.

79. Kim T, Lee JH, Lee H, et al. An area-average approach to peening residual stress under multi-impacts using a three-dimensional symmetry-cell finite element model with plastic shots. *Mater Design* 2010; 31: 50–59.

80. Ahmadi M, Sadeghi BM, Irani M, et al. Finite element simulation of shot peening of an aluminum alloy considering hardening models. *Russ J Non Ferr Met +* 2016; 57: 565–571.

81. Han K, Peric D, Owen DRJ, et al. A combined finite/discrete element simulation of shot peening processes – part II: 3D interaction laws. *Eng Computation* 2000; 17: 680–702.

82. Sherafatnia K, Farrahi GH, Mahmoudi AH, et al. Experimental measurement and analytical determination of shot peening residual stresses considering friction and real unloading behavior. *Mat Sci Eng A: Struct* 2016; 657: 309–321.

83. Taro M, Chaise T and Nélias D. A methodology to predict the roughness of shot peened surfaces. *J Mater Process Tech* 2015; 217: 65–76.

84. Meguid SA, Shagal G and Stranart JC. Finite element modelling of shot-peening residual stresses. *J Mater Process Tech* 1999; 92–93: 401–404.

85. Meguid SA, Shagal G, Stranart JC, et al. Three-dimensional dynamic finite element analysis of shot-peening induced residual stresses. *Finite Elem Anal Des* 1999; 31: 179–191.

86. Johnson W. *Impact strength of materials*. London: Edward Arnold, 1972, pp.264–265.

87. Fathallah R, Inglebert G and Castex L. Determination of shot peening coefficient of restitution. *Surf Eng* 2003; 19: 109–113.

88. Mori KI, Osakada K and Matsuoka N. Rigid-plastic finite element simulation of peening process with plastically deforming shot. *Nihon Kikai Gakkai Ronbunshu A Hen/Trans Jpn Soc Mech Eng Part A* 1995; 61: 1337–1343.

89. Miao HY. *Numerical and theoretical study of shot peening and stress peen forming process*. Montreal, QC, Canada: Ecole Polytechnique, 2010.

90. Xie L, Wang C, Wang L, et al. Numerical analysis and experimental validation on residual stress distribution of titanium matrix composite after shot peening treatment. *Mech Mater* 2016; 99: 2–8.

91. Farrahi GH, Lebrun JL and Couratin D. Effect of shot peening on residual-stress and fatigue life of a spring steel. *Fatigue Fract Eng M* 1995; 18: 211–220.

92. Curtis S, de los Rios ER, Rodopoulos CA, et al. Analysis of the effects of controlled shot peening on fatigue damage of high strength aluminium alloys. *Int J Fatigue* 2003; 25: 59–66.

93. Elbella A, Rami V and Hogirala J. A sensitivity analysis of shot peening parameters. In: *ASME 2006 international design engineering technical conferences & computers and information in engineering conference (IDETC/CIE)*, Philadelphia, PA, 10–13 September 2006, pp.1003–1010. New York: ASME.

94. Tekeli S. Enhancement of fatigue strength of SAE 9245 steel by shot peening. *Mater Lett* 2002; 57: 604–608.

95. Kyriacou S. Shot peening mechanics, a theoretical study. In: *The 6th international conference on shot peening* (ed J Champaigne), San Francisco, CA, 2–5 September 1996, pp.505–516. Mishawaka: Electronics Inc.

96. Schwarzer J, Schulze V and Vohringer O. Finite element simulation of shot peening – a method to evaluate the influence of peening parameters on surface characteristics. In: *The 8th international conference on shot peening* (ed L Wagner), Garmisch-Partenkirchen, 16–20 September 2002. Weinheim: Wiley-VCH.

97. SAE standard J2277:2003. Shot peening coverage. Surface vehicle recommended practice.

98. Baragetti S. Three-dimensional finite-element procedures for shot peening residual stress filed prediction. *Int J Comput Appl T* 2001; 14: 51–63.

99. Jianming W, Feihong L, Feng Y, et al. Shot peening simulation based on SPH method. *Int J Adv Manuf Tech* 2011; 56: 571–578.

100. Zhan K, Jiang CH and Ji V. Uniformity of residual stress distribution on the surface of S30432 austenitic stainless steel by different shot peening processes. *Mater Lett* 2013; 99: 61–64.

101. Rousseau T, Hoc T, Gilles P, et al. Effect of bead quantity in ultrasonic shot peening: surface analysis and numerical simulations. *J Mater Process Tech* 2015; 225: 413–420.

102. Almen JO, Black PH and Dolan TJ. *Residual stresses and fatigue in metals*. New York: McGraw-Hill, 1963, p.368.

103. Vielma AT, Llaneza V and Belzunce FJ. Shot peening intensity optimization to increase the fatigue life of a quenched and tempered structural steel. *Proced Eng* 2014; 74: 273–278.

104. Karuppanan S, Romero JS, de los Rios ER, et al. A theoretical and experimental investigation into the development of coverage in shot peening. In: Wagner IL (ed.) *Shot peening*. Weinheim: Wiley-VCH, 2002, pp.101–107.

105. Rybakov GM. Energy saturation of metal parts by surface plastic deformation. *Russ Eng Res* 2007; 27: 362–364.

106. Tu F, Delbergue D, Miao H, et al. A sequential DEM-FEM coupling method for shot peening simulation. *Surf Coat Tech* 2017; 319: 200–212.

107. Unal O. Optimization of shot peening parameters by response surface methodology. *Surf Coat Tech* 2016; 305: 99–109.

108. Huang X, Liu Z and Xie H. Recent progress in residual stress measurement techniques. *Acta Mech Solida Sin* 2013; 26: 570–583.

109. Romero JS, De Los Rios ER, Levers A, et al. Towards the optimisation of the shot peening process in terms of fatigue resistance of the 2024-T351 and 7150-T651 aluminium alloys. *WIT Trans Eng Sci* 2001; 33: 343–355.

110. Evans RW. Shot peening process: modelling, verification, and optimisation. *Mater Sci Tech* 2002; 18: 831–839.

111. Kirk D. Work-hardening during peening. *Shot Peen* 2017; 31, https://www.shotpeener.com/library/pdf/2017024.pdf

112. Kirk D. Peening intensity curves. *Shot Peen* 2007; 21: 24–30, https://www.shotpeener.com/library/pdf/2007020.pdf

113. Kirk D. Almen strip quality. *Shot Peen* 2018; 32: 26–36.

114. Levers A, Romero JS, Rios E, et al. Optimisation of the shot peening process in terms of fatigue resistance. In: Nakonieczny A (ed.) *The 7th international conference on shot peening*. 1999, pp.117–126. Mishawaka: Electronics Inc.

115. Petit-Renaud F, Evans JT, Metcalfe AV, et al. Optimization of a shot peening process. *Proc IMechE, Part L: J Materials: Design and Applications* 2008; 222: 277–289.

116. Cammett JT, Prevey PS and Jayaraman N. The effect of shot peening coverage on residual stress, cold work, and fatigue in a nickel-base superalloy. In: *Proceedings of the 9th international conference for shot peening* (ICSP 9) (eds V Schulze and A Niku-Lari), Paris, 6–9 September 2005, pp.295–304. Mishawaka: Electronics Inc.

117. Nam YS, Jeon U, Yoon HK, et al. Use of response surface methodology for shot peening process optimization of an aircraft structural part. *Int J Adv Manuf Tech* 2016; 87: 2967–2981.

118. Hu K, Wu J, Wang T, et al. Numerical simulation and parameter optimization for shot peen forming process based on temperature gradient. *China Mech Eng* 2007; 18: 292–295.

119. Caramia M and Dell'Olmo P. *Multi-objective optimization. Multi-objective management in freight logistics*. London: Springer, 2008.

120. Belegundu AD and Chandrupatla TR. *Optimization concepts and applications in engineering*. New York: Cambridge University Press, 1999.

121. Marsh KJ. *Shot peening: techniques and applications*. Warley: Engineering Materials Advisory Service Ltd, 1993.

122. SAE standard J444:1993. Surface vehicle recommended practice.

123. Xie L, Zhang J, Xiong C, et al. Investigation on experiments and numerical modelling of the residual stress distribution in deformed surface layer of Ti-6Al-4V after shot peening. *Mater Design* 2012; 41: 314–318.

124. Barrett C and Todd R. Investigation of the effects of elastic pre-stressing technique on magnitude of compressive residual stress induced by shot peen forming of thick aluminum plates. In: *Proceedings of the 2nd international conference on shot peening*. Chicago, IL, 14–17 May 1984, pp.15–21. Mishawaka: Electronics Inc.

125. Champaigne J. Shot peening overview. *Shot Peen* 2001, https://www.shotpeener.com/library/pdf/2001012.pdf

126. Seo TI, Song BU and Jeong YS. Optimization of shot-peening conditions and wave profiles to improve durability of wave cushion spring. In: *The 3rd international conference on advanced engineering materials and technology* (AEMT), Zhangjiajie, China, 11–12 May 2013, pp.2287–2290. California: Trans Tech Publications.

127. Kleijnen JPC. *Design and analysis of simulation experiments*. New York: Springer, 2015.

128. Baragetti S, Guagliano M and Vergani L. A numerical procedure for shot peening optimization by means of non-dimensional factors. *Int J Mater Prod Tec* 2000; 15: 91–103.